



## THE INFLUENCE OF TEMPERATURE ON THE QUALITY OF GAS FLUIDIZATION

S. RAPAGNÁ,<sup>1</sup> P. U. FOSCOLO<sup>1</sup> and L. G. GIBILARO<sup>2</sup>

<sup>1</sup>Department of Chemistry, Chemical Engineering and Material Science, University of L'Aquila, 67100 L'Aquila, Italy

<sup>2</sup>Department of Chemical and Biochemical Engineering, University College London, London WC1E 7JE, England

(Received 23 May 1993; in revised form 19 October 1993)

**Abstract**—Results are presented of an experimental study of the effect of temperature (up to 910°C) on the fluidization characteristics of three powders, chosen to span the fine-to-moderate size range. The major conclusions are that: the onset of bubbling, as measured by the minimum bubbling voidage, is progressively delayed with increasing temperature—in good agreement with theoretical predictions; and the quality of fluidization in the bubbling regime, quantified in terms of the standard deviation of bed pressure fluctuations, may be predicted for elevated-temperature systems from experiments conducted under ambient conditions.

**Key Words:** fluidization, minimum bubbling point, effect of temperature

### 1. INTRODUCTION

Gas fluidized beds of fine powders (particle diameter,  $d_p$ , less than about 100  $\mu\text{m}$ ) are mainly employed as catalytic chemical reactors, often operating under high-temperature, and sometimes also high-pressure, conditions (Kunii & Levenspiel 1991). Because of their importance in industrial applications, the fluidization characteristics of such systems have been studied widely, with special attention being paid to the effect of particle density and size range on the enhancement of gas-solid contact and, as a consequence, chemical conversion (Geldart 1973; Rowe *et al.* 1978; Grace & Sun 1991).

Given that most of the experimental data available from the literature are obtained under ambient conditions, it is important to evaluate the influence of process variables such as temperature, in order to arrive at appropriate scale-up design procedures. We have shown previously that dynamic similarity rules of the type first proposed by Glicksman (1984) for moderate-size particle systems ( $d_p$  between about 100 and 1000  $\mu\text{m}$ ) are also applicable to fine catalyst fluidization (Foscolo *et al.* 1991; Rapagná *et al.* 1992), thereby extending the validity of hydrodynamic scaling to such systems. This generalization led to a theoretical powder classification map for fluidization by any fluid (Foscolo *et al.* 1991), in good agreement with empirical diagrams proposed by Geldart (1973) and Grace (1986). The model providing the basis for this map predicts a substantial influence of the operating temperature, specifically on the minimum bubbling point (i.e. the bed void fraction value marking the transition from homogeneous to bubbling behaviour), which is traditionally considered the characterizing feature of fine powder fluidization. As previously pointed out (Gibilaro *et al.* 1988), temperature remains the only process variable for which insufficient data are available in the literature to thoroughly test the model predictions. The main purpose of this work has been to acquire significant experimental evidence on this point, over a wide temperature range (ambient up to about 900°C).

### 2. EXPERIMENTAL

Figure 1 illustrates the experimental apparatus used in this study. The particles were contained in a cylindrical steel vessel of i.d. = 50 mm and supported on a porous alumina distributor plate;

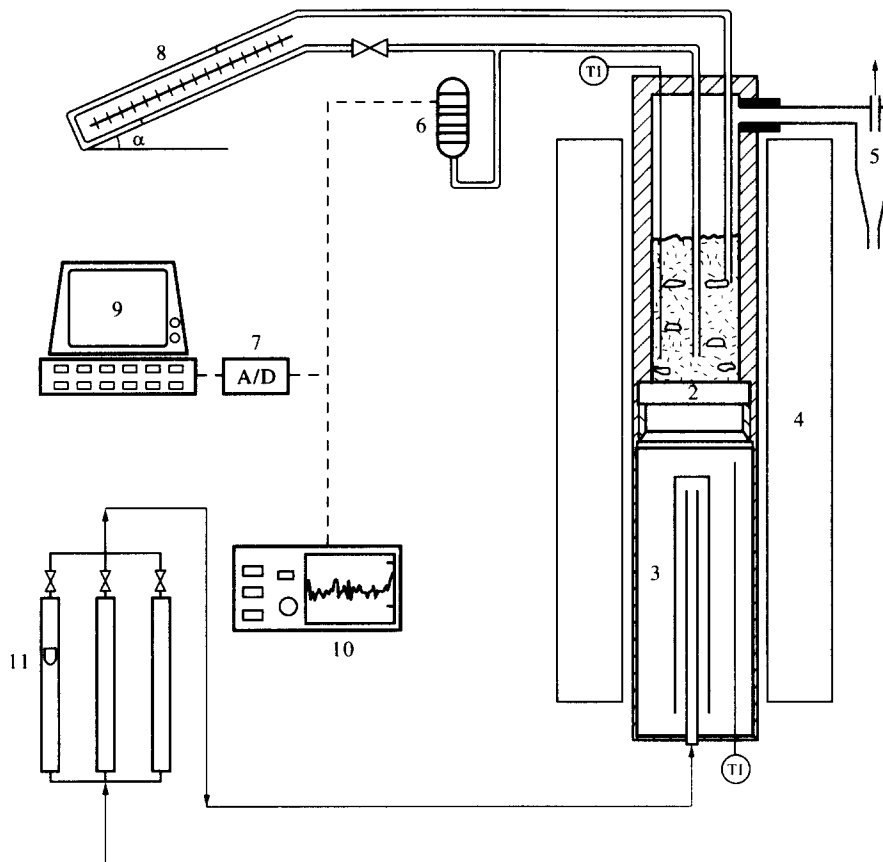


Figure 1. Scheme of the experimental apparatus: 1, fluidized bed; 2, porous plate distributor; 3, windbox; 4, electric furnace; 5, cyclone; 6, piezoelectric sensor; 7, data acquisition interface; 8, water manometer; 9, PC; 10, oscilloscope; 11, rotameter bench.

the bed height was about 170 mm. The bed was heated to the operating temperature by means of a cylindrical electric furnace in which the bed container was placed.

The furnace available determined the choice of the bed diameter. Experimental tests carried out at room temperature with 100 and 150 mm i.d. columns showed no influence of the bed diameter on the measured quantities—specifically the minimum fluidization and minimum bubbling point—for all the powder samples used in this study. It is also worth noting that the values observed for the minimum fluidization voidage,  $\epsilon_{mf}$ , were always close to 0.4 and therefore any effect of the column diameter on the bed packing structure, before fluidization takes place, may be regarded as insignificant in our case.

A tortuous path for the fluidizing gas (nitrogen) in the wind box ensured that the operating temperature was reached before the gas contacted the bed of particles. The gas flow rate was measured at room temperature by means of a rotameter manifold and the volumetric flux at the inlet to the bed,  $u_0$ , was calculated using the ideal gas law.

The following interpolation of tabulated data (Perry 1984) was utilized to estimate the nitrogen viscosity,  $\mu_f$ , as a function of temperature:

$$\mu_f = 1.66 \cdot 10^{-5} \left( \frac{T}{273} \right)^{0.728}, \quad [1]$$

where  $T$  is the temperature, in Kelvin.

The temperature of the furnace inside wall was automatically controlled at a constant uniform value. The temperatures immediately below the distributor plate and just above the bed were recorded by means of two Fe/K thermocouples. This facility enabled temperature fluctuations to be contained within very narrow limits (about 1% of the operating temperature in °C), in spite

of the quite significant changes in the gas flow rate from the fixed bed to the vigorously bubbling fluidization regimes.

Pressure drop measurements,  $\Delta P$ , across both the whole bed and over a certain portion of it ( $\Delta H = 100$  mm) were obtained by means of an inclined water manometer connected to pressure probes: the former measurement enables the minimum fluidization velocity,  $u_{mf}$ , to be determined in the conventional manner, whereas the latter delivers the overall void fraction of the suspension:

$$\epsilon_{av} = 1 - \frac{1}{(\rho_p - \rho_f)g} \frac{\Delta P}{\Delta H}, \quad [2]$$

where  $\rho_p$  and  $\rho_f$  indicate particle and fluid density, respectively, and  $g$  is the gravitational field strength.

The first appearance of bubbles inside the bed was detected by means of a piezoelectric pressure transducer connected to an oscilloscope, as shown in figure 1: this detects, in real time, the occurrence of pressure fluctuations induced by bubbles bursting through the top of the bed. The same instrument was utilized in the bubbling regime to characterize the overall fluidization quality; in this case the voltage signal was logged and analyzed as described by Di Felice *et al.* (1992).

The density, equivalent diameter and size distribution of the powders examined in this study are reported in table 1: sample I is a commercial cracking catalyst; sample II was obtained from sample I by sieving; and sample III is sieved silica sand.

These powders are the same ones as utilized in previous experimental investigations at room temperature under both, ambient and high-pressure conditions; their physical properties have been repeatedly checked by different methods. For example, the particle density of the FCC powders was measured using both, mercury picnometry and the "pouring method" proposed by Geldart (1986); these values were in close agreement and consistent with the bulk density value provided by the manufacturer.

The thermal stability of the three samples over the full temperature range was verified by thermogravimetric analysis: samples I and II (porous particles) showed a weight loss of about 8% as a result of losing adsorbed moisture—the density values in table 1 are corrected for this effect. Before performing the experimental tests, the powder samples were heated to the highest temperature level and then maintained under a dry nitrogen atmosphere until all measurements had been completed.

It is worth noting at this stage that, under ambient conditions, sample I exhibits an initial range of homogeneous expansion, which is typical of systems belonging to group A of the Geldart (1973) classification; on the other hand, samples II and III exhibit bubbling behaviour right from the minimum fluidization condition.

For each of the powders listed in table 1, the minimum fluidization velocity, the minimum bubbling point and the variance of the instantaneous pressure fluctuations in the bubbling regime were observed as functions of temperature. The trends exhibited were compared, where possible, with previous experimental results and theoretical predictions.

Table 1. Size distributions and density of fluidized particles

	Sample I (%)	Sample II (%)		Sample III (%)
> 180 $\mu\text{m}$	0.59	0.92	> 710 $\mu\text{m}$	0.30
180–150 $\mu\text{m}$	1.68	3.15	710–600 $\mu\text{m}$	1.40
150–125 $\mu\text{m}$	6.66	25.20	600–500 $\mu\text{m}$	6.70
125–106 $\mu\text{m}$	6.95	24.80	500–425 $\mu\text{m}$	20.50
106–90 $\mu\text{m}$	10.73	25.60	425–355 $\mu\text{m}$	28.90
90–75 $\mu\text{m}$	13.91	11.08	355–300 $\mu\text{m}$	24.40
75–63 $\mu\text{m}$	14.41	2.85	300–250 $\mu\text{m}$	14.30
63–53 $\mu\text{m}$	18.17	< 63 $\mu\text{m}$ 6.40	< 250 $\mu\text{m}$	3.50
53–45 $\mu\text{m}$	12.32			
45–38 $\mu\text{m}$	10.23			
38–32 $\mu\text{m}$	3.87			
32–26 $\mu\text{m}$	0.39			
< 26 $\mu\text{m}$	0.09			
Equivalent diameter, $d$ ( $\mu\text{m}$ )	65	103		348
Density, $\rho_p$ ( $\text{kg m}^{-3}$ )	1500	1500		2640

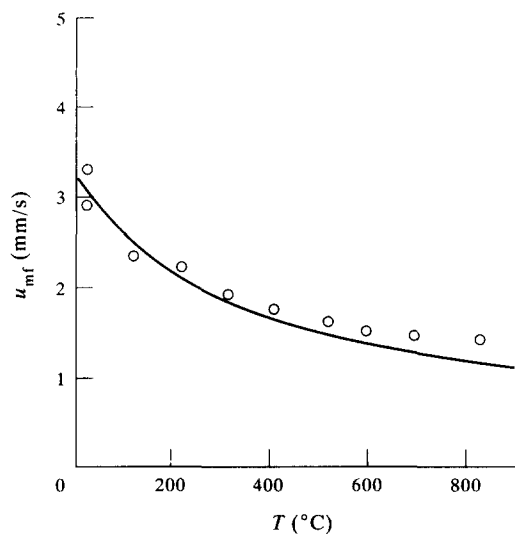


Figure 2. Minimum fluidization velocity as a function of temperature for powder sample I:  $\circ$ , experimental data; —, calculated values with  $\epsilon_{mf} = 0.42$ .

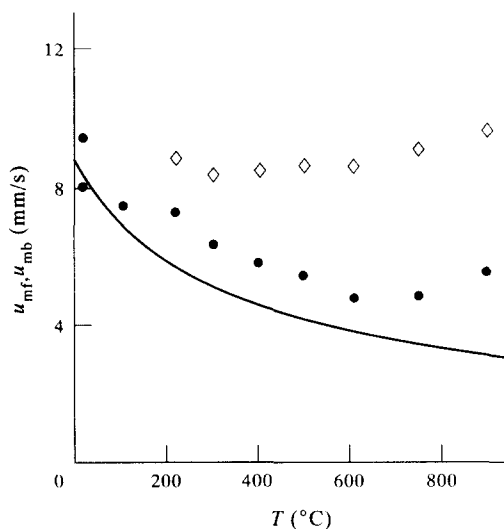


Figure 3. Minimum fluidization and minimum bubbling velocity as a function of temperature for powder sample II:  $\bullet$ , experimental  $u_{mf}$ ;  $\diamond$ , experimental  $u_{mb}$ ; —, calculated values of  $u_{mf}$  with  $\epsilon_{mf} = 0.43$ .

### 3. RESULTS AND DISCUSSION

#### 3.1. Incipient fluidization point

Figures 2–4 show the observed values of the minimum fluidization velocity as functions of temperature; the solid lines represent the predictions obtained with the Ergun equation for particles of spherical shape and for the value of minimum fluidization voidage,  $\epsilon_{mf}$ , measured under ambient conditions. In all cases the experimental  $u_{mf}$  decreases with increasing temperature, because of the controlling effect of gas viscosity in the Reynolds number range relevant for this study, but somewhat less than could be inferred from consideration of the change in the gas properties alone.

This conclusion is in agreement with that of a previous investigation by Botterill *et al.* (1982), carried out with particles of larger size ( $d_p = 380$  to  $2320 \mu\text{m}$ ); our findings show that the influence of temperature on the minimum fluidization velocity, as described by these authors, also applies to fine catalyst fluidized systems.

It should be pointed out that, in order to obtain reproducible results for the incipient fluidization point, it is important to operate in a carefully-controlled manner: a sudden change in the gas velocity, for example, can give rise to significant modifications in the structure of the fixed bed and, as a consequence, affect the  $\epsilon_{mf}$  values. This sensitivity to the history of the measurement procedure appears progressively more pronounced with increasing temperature, possibly as a result of an increase in particle–particle friction which would lead to an increase in particle bridging, and hence higher packed bed void fractions, on defluidization, as has recently been reported by Raso *et al.* (1992), particularly in relatively small diameter beds. This could explain the progressive deviations from the predictions of the Ergun equation for increasing temperatures reported in figures 2–4: the greatest discrepancy occurs with sample II at the highest operating temperature, where an  $\epsilon_{mf}$  value of about 0.50 (rather than the measured ambient value of 0.43) is required to match the predictions.

#### 3.2. Minimum bubbling point

As indicated above, the evaluation of the minimum bubbling point conditions represents the major aim of this investigation. This condition was detected in a number of ways that provided consistent measurements of  $\epsilon_{mb}$ .

Fluctuations of the pressure drop across the whole bed were observed by replacing the water manometer, used for minimum fluidization point detection, with a fast-responding piezoelectric transducer connected to an oscilloscope. This shows quite clearly the commencement of bubbling: on gradually increasing the gas flow rate, a point is reached where relatively high frequency

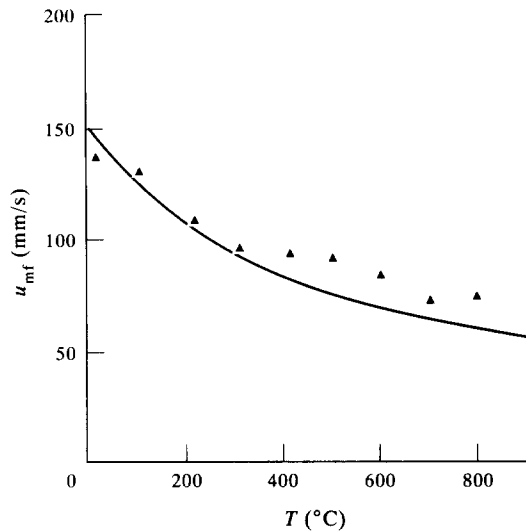


Figure 4. Minimum fluidization velocity as a function of temperature for powder sample III:  $\blacktriangle$ , experimental data; —, calculated values with  $\epsilon_{mf} = 0.42$ .

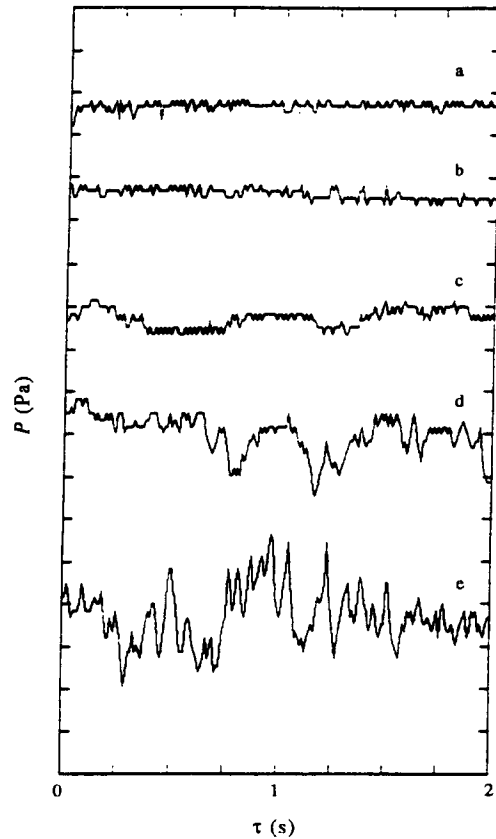


Figure 5. Pressure fluctuations at and near  $u_{mb}$  for sample II at 520°C: (a)  $u_0 = 3.5$  mm/s; (b)  $u_0 = 5.5$  mm/s; (c)  $u_0 = 7.5$  mm/s; (d)  $u_0 = 8.5$  mm/s; (e)  $u_0 = 9.5$  mm/s.

oscillations (in the 5–10 Hz range) appear and rapidly increase in amplitude; a gradual reduction in the flow rate identifies the same point at which these oscillations rapidly decrease—a typical reproduction of this behaviour is illustrated in figure 5. This procedure identifies the minimum bubbling velocity,  $u_{mb}$ .

The above procedure was repeated for fluctuations in pressure across the internal 100 mm of bed, after the water manometer had been used to monitor the pressure drop profile with gas velocity: the sudden change in oscillation amplitude, that occurred at the same point for both increasing and decreasing gas velocities, corresponded to that found previously in every case.

In some cases it was possible to identify the minimum bubbling point from a local minimum in the  $\Delta P$  vs  $u$  relationship for the fixed 100 mm of bed: as the gas velocity is increased across the minimum bubbling value, homogeneous expansion gives way to bed partial collapse and hence a local minimum in  $\Delta P$ . Figure 6(b) illustrates this phenomenon for sample I under ambient conditions: the  $u_{mb}$  value shown was determined from pressure fluctuations, as described above, and will be seen to correspond to the shallow minimum observed. An effect of high temperature appears to be a decrease in bed collapse, as is certainly the case for high-pressure operation (Jacob & Weimer 1988): this is illustrated in figure 7 for sample II at 910°C, where no minimum at  $u_{mb}$  is apparent.

Figures 8 and 9 show observed values of  $\epsilon_{mb}$  for samples I and II, respectively, and also predictions of the particle bed model (Foscolo & Gibilaro 1984): in both cases the trend with temperature follows the model predictions reasonably well. The sample II results are particularly interesting, as they represent group B behaviour (bubbling from the minimum fluidization point) up to a temperature somewhat in excess of 100°C and thereafter an initial regime of homogeneous fluidization up to the minimum bubbling point (group A): as is clear from figure 9, this feature is in close accord with the model predictions.

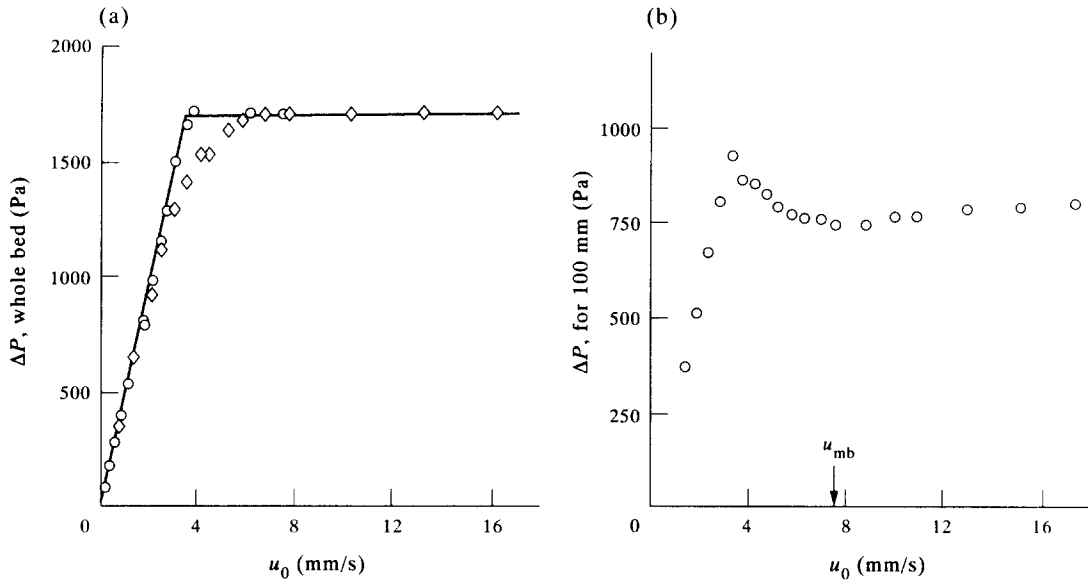


Figure 6. Sample I at 20°C: (a) experimental determination of the minimum fluidization velocity; (b) experimental determination of the minimum bubbling voidage. With increasing (○) and decreasing (◇) gas flow rate.

3.3. Bubbling regime

As is well-known, the pattern of the instantaneous pressure fluctuations, detected at a given height inside the bed, provides an overall measure of “fluidization quality” in the bubbling regime, although a precise correspondence with the characteristics of individual bubbles is difficult to obtain. This phenomenon has been successfully utilized in comparisons of different systems when scale-up rules are applied (Di Felice *et al.* 1992). In what follows, the results obtained at different temperatures and fluidizing velocities, for each of the powders listed in table 1, are presented in terms of the standard deviation of the pressure signal,  $\sigma$ , a variable that is sensitive to the operating conditions.

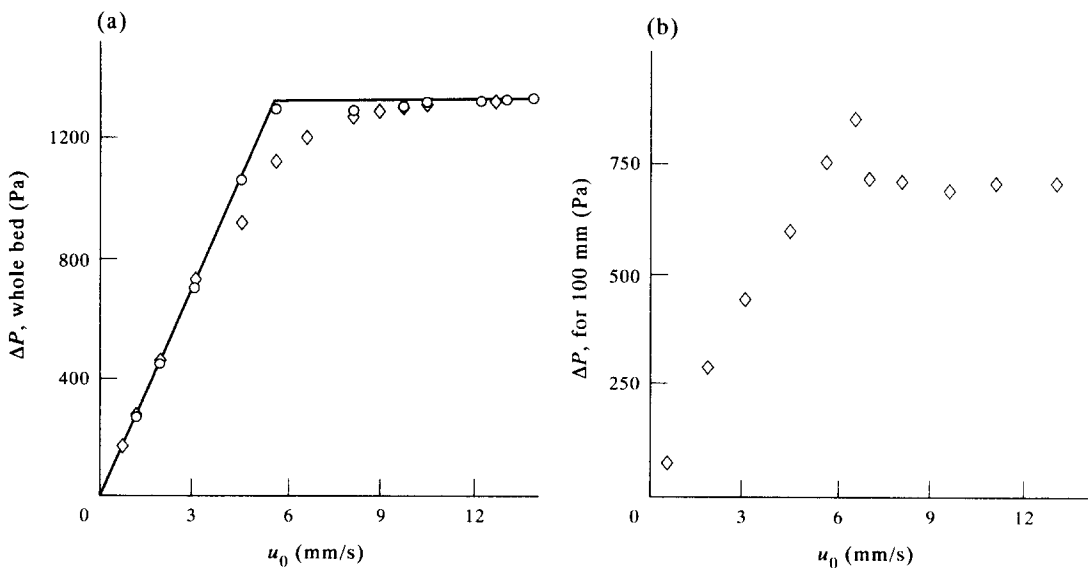


Figure 7. Sample II at 910°C: (a) experimental determination of the minimum fluidization velocity; (b) experimental determination of the minimum bubbling voidage. With increasing (○) and decreasing (◇) gas flow rate.

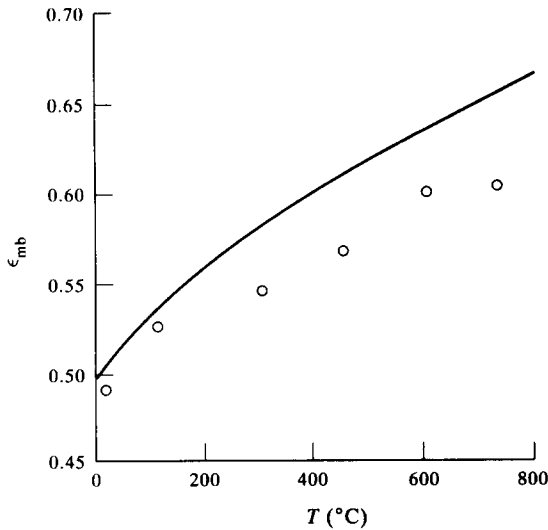


Figure 8. Experimental and calculated values of  $\epsilon_{mb}$  as a function of temperature for sample I.

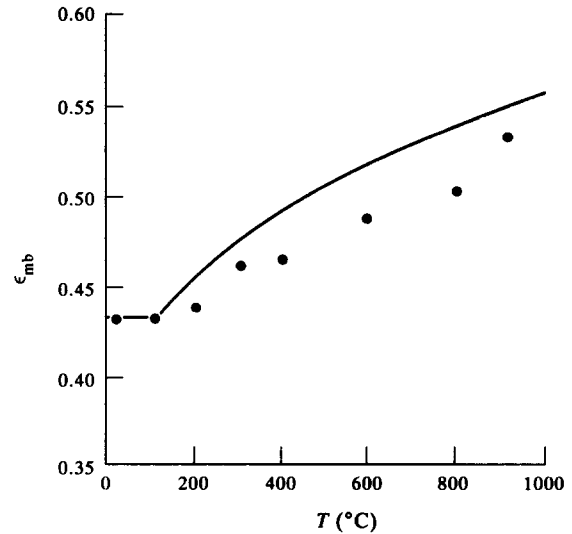


Figure 9. Experimental and calculated values of  $\epsilon_{mb}$  as a function of temperature for sample II.

Figures 10–12 illustrate the trends obtained for this quantity, as a function of the excess gas velocity  $u - u_{mf}$ . It is important to stress that the numerical values obtained with different powders cannot be compared with each other, because the overall bed height and the relative position of the pressure probe are different for each case.

With the sand powder,  $d_p = 348 \mu\text{m}$ , the standard deviation of the pressure fluctuations does not change very much with temperature over the whole range of variation of the fluidizing velocity. On the other hand, with sample II ( $d_p = 103 \mu\text{m}$ ) and even more markedly with the finest powder (sample I,  $d_p = 65 \mu\text{m}$ ), temperature has the general effect of appreciably reducing the intensity of the pressure fluctuations at the same excess flow, indicating a significant decrease in the average bubble size; moreover, a delay in bubble development is also evident, and corresponds to the extended homogeneous expansion range at low fluidizing velocities.

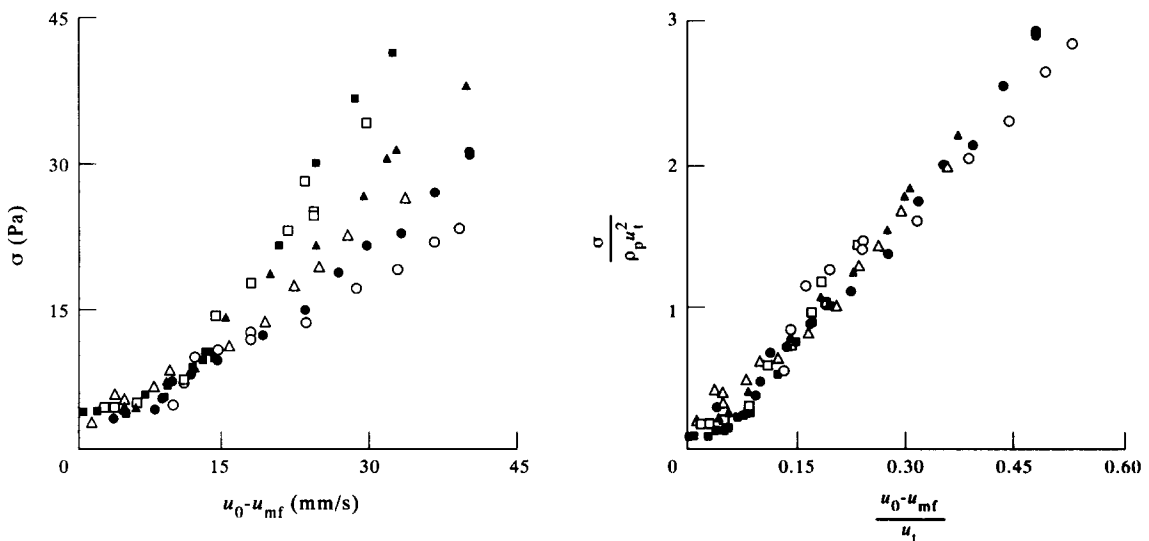


Figure 10. Sample I—the standard deviation of the pressure signal as a function of the excess gas velocity, at different temperatures: ■, 24°C; □, 205°C; ▲, 354°C; △, 497°C; ●, 639°C; ○, 836°C. Right-hand side diagram: dimensionless form.

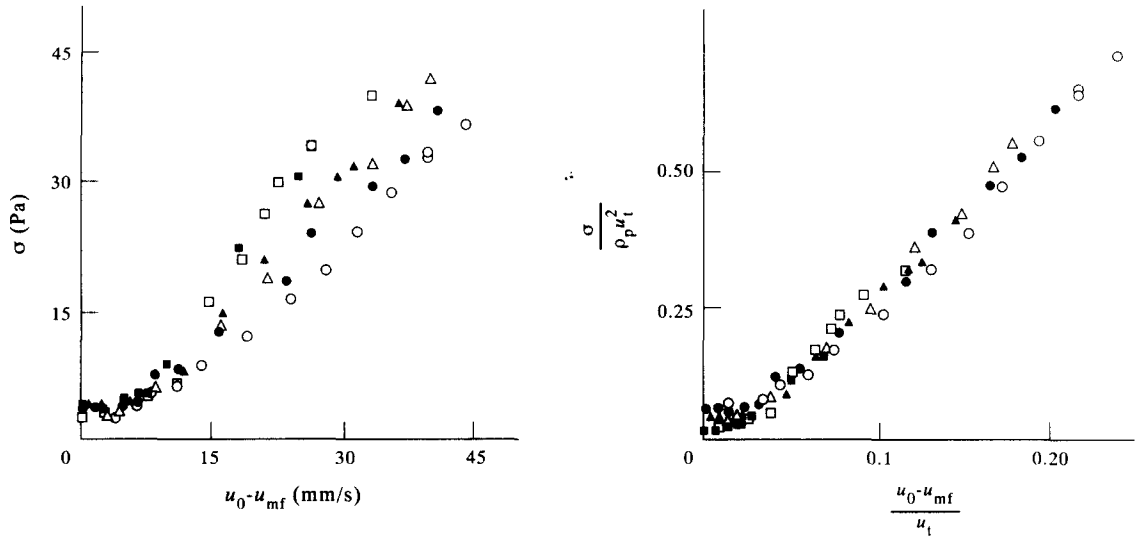


Figure 11. Sample II—the standard deviation of the pressure signal as a function of the excess gas velocity, at different temperatures: ■, 15°C; □, 208°C; ▲, 354°C; △, 492°C; ●, 635°C; ○, 784°C. Right-hand side diagram: dimensionless form.

Also shown in figures 10–12 are the same data in dimensionless form, the pressure standard deviation and the gas velocity being divided by  $\rho_p u_t^2$  and  $u_t$ , respectively;  $u_t$  is the particle terminal settling velocity, which has been conveniently calculated as reported by Foscolo & Gibilaro (1984). These quantities have been chosen according to similarity rules previously developed and referred to above. An interesting result is obtained: for each powder, all the experimental data are well-correlated by a single line. This indicates that for the systems examined here the fluidization quality, at a given temperature and fluidizing velocity, can be inferred from a knowledge of the bed behaviour under ambient conditions.

#### 4. CONCLUSIONS

The influence of temperature (up to about 900°C) on the behaviour of fluidized beds has been investigated experimentally: its effect on the minimum fluidization and minimum bubbling

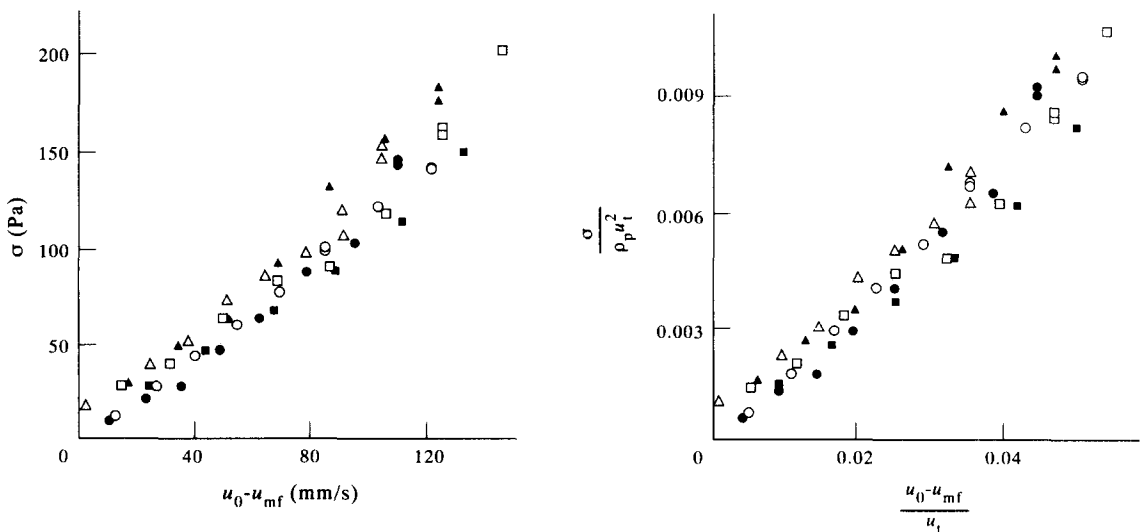


Figure 12. Sample III—the standard deviation of the pressure signal as a function of the excess gas velocity, at different temperatures. ■, 18°C; □, 200°C; ▲, 342°C; △, 503°C; ●, 661°C; ○, 787°C. Right-hand side diagram: dimensionless form.



conditions, as well as on the overall bubbling pattern, has been quantified for both fine- and moderate-size powder systems.

The reduction of the minimum fluidization velocity with temperature is less severe than that which could be predicted with reference to the corresponding changes taking place in the gas properties, and almost negligible for temperatures  $>400^{\circ}\text{C}$  with fine catalysts.

The minimum bubbling voidage increases with temperature, in good agreement with the predictions of the particle bed model (Foscolo & Gibilaro 1984). As the temperature is increased, a well-defined range of homogeneous bed expansion may appear with a powder which is characterized by purely heterogeneous behaviour under ambient conditions.

The standard deviation of the pressure fluctuations in the bubbling regime is not affected appreciably by temperature in the case of the moderate-size particle system, whereas with smaller particles its value reduces noticeably as the temperature is increased from ambient to  $850^{\circ}\text{C}$ , over a wide range of gas velocities. The experimental data for a particular bed correlate well in a temperature-dependent manner when plotted in dimensionless coordinates.

Finally, with fine powder systems, the results obtained imply that the porosity of the dense phase increases and the average bubble size decreases with temperature; both these phenomena have a positive effect on enhancing chemical conversion for the case of active catalysts.

*Acknowledgement*—The authors would like to acknowledge the financial support of the Consiglio Nazionale delle Ricerche under their specially promoted programme "Chimica Fine".

#### REFERENCES

- BOTTERILL, J. S. N., TEOMAN, Y. & YUREGIR, K. R. 1982 The effect of operating temperature on the velocity of minimum fluidization, bed voidage and general behaviour. *Powder Technol.* **31**, 101–110.
- DI FELICE, R., RAPAGNÁ, S. & FOSCOLO, P. U. 1992 Dynamic similarity rules: validity check for bubbling and slugging fluidized beds. *Powder Technol.* **71**, 281–287.
- FOSCOLO, P. U. & GIBILARO, L. G. 1984 A fully predictive criterion for the transition between particulate and aggregate fluidization. *Chem. Engng Sci.* **39**, 1667–1675.
- FOSCOLO, P. U., GIBILARO, L. G. & DI FELICE, R. 1991 Hydrodynamic scaling relationships for fluidization. In *Computational Fluid Dynamics for the Petrochemical Process Industry*. Kluwer, Dordrecht, The Netherlands.
- GELDART, D. 1973 Types of gas fluidization. *Powder Technol.* **7**, 285–292.
- GELDART, D. 1986 *Gas Fluidization Technology*, pp. 17–18. Wiley, Chichester, U.K.
- GIBILARO, L. G., DI FELICE, R. & FOSCOLO, P. U. 1988 On the minimum bubbling voidage and the Geldart classification for gas-fluidized beds. *Powder Technol.* **56**, 21–29.
- GLICKSMAN, L. R. 1984 Scaling relationships for fluidized beds. *Chem. Engng Sci.* **39**, 1373–1379.
- GRACE, J. R. 1986 Contacting modes and behaviour of gas–solid and other two-phase suspensions. *Can. J. Chem. Engng* **64**, 353–363.
- GRACE, J. R. & SUN, G. 1991 Influence of particle size distribution on the performance of fluidized bed reactors. *Can. J. Chem. Engng* **69**, 1126–1134.
- JACOB, K. V. & WEIMER, A. W. 1988 Normal bubbling of fine carbon powders in high-pressure fluidized beds. *AIChE JI* **34**, 1395–1397.
- KUNII, D. & LEVENSPIEL, O. 1991 *Fluidization Engineering*. Butterworth–Heinemann, London.
- PERRY, R. H. 1984 *Chemical Engineering Handbook*. McGraw–Hill, New York.
- RAPAGNÁ, S., DI FELICE, R., FOSCOLO, P. U. & GIBILARO, L. G. 1992 Experimental verification of the scaling rules for fine powder fluidization. In *Fluidization VII*, pp. 579–586. Engng Foundation, New York.
- RASO, G., D'AMORE, M., FORMISANI, B. & LIGNOLA, P. G. 1992 The influence of temperature on the properties of the particulate phase at incipient fluidization. *Powder Technol.* **72**, 71–76.
- ROWE, P. N., SANTORO, L. & YATES, J. G. 1978 The division of gas between bubble and interstitial phases in fluidised beds of fine powders. *Chem. Engng Sci.* **33**, 133–140.